



HAL
open science

Nanoscale optical trap for fluorescent nanoparticles

Olivier Emile, Janine Emile, Hervé Tabuteau

► **To cite this version:**

Olivier Emile, Janine Emile, Hervé Tabuteau. Nanoscale optical trap for fluorescent nanoparticles. EPL - Europhysics Letters, 2020, 129 (5), pp.58001. 10.1209/0295-5075/129/58001 . hal-02862822

HAL Id: hal-02862822

<https://univ-rennes.hal.science/hal-02862822>

Submitted on 17 Jun 2020

HAL is a multi-disciplinary open access archive for the deposit and dissemination of scientific research documents, whether they are published or not. The documents may come from teaching and research institutions in France or abroad, or from public or private research centers.

L'archive ouverte pluridisciplinaire **HAL**, est destinée au dépôt et à la diffusion de documents scientifiques de niveau recherche, publiés ou non, émanant des établissements d'enseignement et de recherche français ou étrangers, des laboratoires publics ou privés.

Nanoscale optical trap for fluorescent nanoparticles.

O. EMILE¹, J. EMILE² and H. TABUTEAU²

¹ *Université de Rennes 1, Campus de Beaulieu, F-35000 Rennes, France*

² *Université de Rennes 1, CNRS IPR UMR 6251, F-35000 Rennes, France*

PACS 87.80.Cc – Optical trapping

PACS 42.50.Wk – Mechanical effects of light on material media, microstructure and particles in optics

PACS 78.45.+h – Stimulated emission

Abstract – Optical trapping has offered new potentialities in the manipulation of bacteria, living cells, organelles, or microparticles in micrometric volumes. Its extension to the nanometer scale may create exceptional opportunities in many areas of science. We report here the trapping of a single 100-nm-radius particle in a nanometric volume. The trapping relies on stimulated emission of the fluorescent particle in the evanescent wave of a totally reflected Arago spot on a glass-liquid interface. The trapping volume is a 200-nm-height and 125-nm-radius cylinder. Such a nano-trap, aside from applications in nano-physics, may echo the needs of life scientists to manipulate ever-smaller biological samples.

Introduction . – The advent of optical tweezers has led to a real revolution in optical manipulation [1] that has spurred a new area of medical, biophysical and physics discovery. This non-contact manipulation technique enables mechanical force measurements [2, 3], 3D micropositioning [4], micro-fabrication assembly [1, 5], cell sorting [6], tissue engineering [7], to name a few. Nevertheless, direct manipulation of matter at the nanometer scale remains a significant challenge for optical tweezers [8], because, on the one hand, the traps are micrometer size limited [9], and on the other hand, because the trapping force diminishes as the third power of the particle diameter [10–12].

Two main directions have been followed to circumvent these limitations [13]. The first one combines tight light focusing and total internal reflection [14–18]. However, whereas the trap size is then in the nanometer range in the direction of the evanescent wave, it is still limited by diffraction in the other directions. The other one uses plasmon enhanced electromagnetic field to break the diffraction limit [19–23]. This can be realized for example, at the end of an optical fibre [24, 25]. Alternatively, polystyrene nano-spheres have been trapped on nanostructured substrates or plasmonic nanopores [26], as well as molecules of biological interest [27], or metallic particles [12]. Nevertheless, these nanometric optical tweezers are based on dedicated plasmonic structures. Versatile nanometer size optical traps are still lacking.

Experimental set-up. – In order to address this challenge, we propose to trap nanoparticles using an Arago spot [28] (Fig. 1a) that experiences total internal reflection at a glass-liquid interface. Whereas Gaussian beams are diffraction limited to a fraction of wavelength, such Arago spots can have smaller sizes. The intensity distribution can be written as [29]

$$I(r) = I_0 \frac{h^2}{h^2 + (d/2)^2} J_0^2\left(\frac{\pi r d}{\lambda(h^2 + (d/2)^2)^{1/2}}\right) \quad (1)$$

J_0 being the zeroth order Bessel function of the first kind, h the distance between the disk and the glass-liquid interface (h equals the thickness of a BK7 glass lamella, $h = 170 \mu\text{m}$), r the distance to the beam axis, λ the light wavelength, d the disk diameter (see Fig. 1a) and I_0 the intensity of the incoming light at the edges of the disk. The maximum light intensity of the spot at the interface is of the order of $I(r = 0) = 100 \text{ mW}\cdot\text{mm}^{-2}$. We characterize its size by its waist w_0 , as for Gaussian beams. It is the radius at which the intensity values fall to $1/e^2$ of its axial value. It here equals to $w_0 = 120 \text{ nm}$, which would be half of the waist of a Gaussian beam of the same wavelength, focused by a lens of numerical aperture equal to 1. However, in the case of a Gaussian beam, there is a large spreading of the direction of the wavevector, whereas, in our case, the angle between the direction of propagation and the wavevectors is constant. The wavevectors lie on a cone.

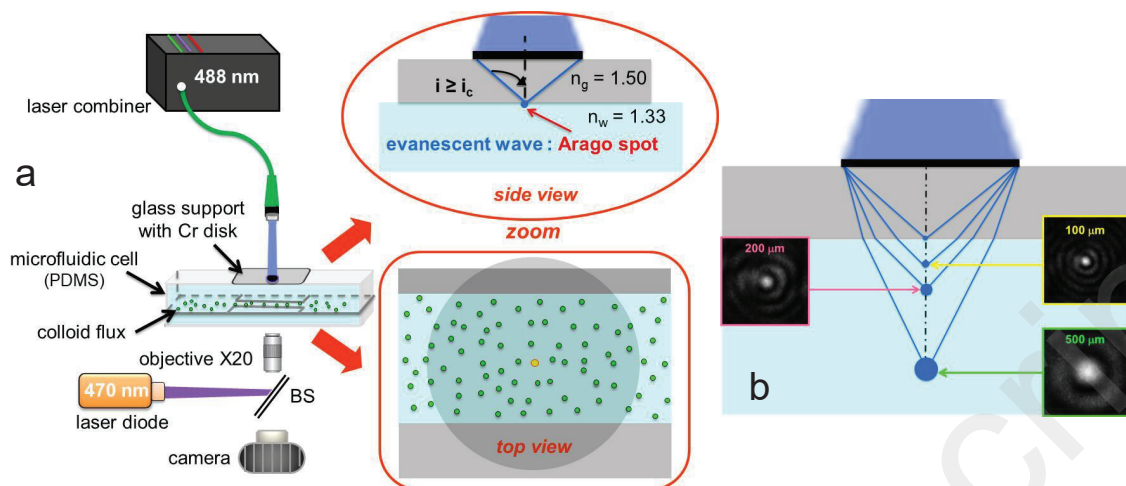


Fig. 1: a) Fluorescent particles (Molecular Probes, diameter $2a = 200$ nm) suspended in water, flowing in a $30 \mu\text{m}$ -height, $300 \mu\text{m}$ -width PDMS (PolyDiMethylSiloxane) micro-channel made by standard soft lithography [30] covered with a glass lamella. The flow can be varied and controlled with a microfluidic pump. The particles are excited from underneath with an optical diode (ThorLabs M470L2, 470 nm central wavelength, power 700 mW, focused to a 1 mm diameter spot on the channel), and trapped in an Arago spot laser originating from the interference of a collimated laser beam (L4Cc Oxxius, wavelength $\lambda = 488$ nm, power 250 mW at the end of an optical fibre) diffracted by the edges of a $d = 650 \mu\text{m}$ chromium occulting disk deposited on a glass substrate. We use an inverted microscope (Leica, X20 objective lens, NA 0.4) equipped with a motorized XY stage. Pictures are taken every 30 ms by a SCMOS monochrome gray-scale camera (Orca flash 4.0 Hamamatsu) and analyzed using ImageJ software [31]. i : angle of incidence, i_c : critical angle. b) Propagation of the Arago spot in the liquid medium that enables the localization of the spot.

53 In order for the Arago spot to be under total internal
 54 reflection conditions, the angle of incidence i of the
 55 diffracted light by the disk ($i = \tan^{-1}(d/2h) = 62.39^\circ$) is
 56 higher than the critical angle $i_c = \sin^{-1}(n_w/n_g) = 61.74^\circ$,
 57 $n_w = 1.33$ and $n_g = 1.51$ being the optical index of
 58 water and glass, respectively. The fluorescent particles
 59 consist of $N = 1.1 \times 10^5$ fluorescein molecules (lifetime
 60 $\tau_f = 4.1$ ns), leading to a fluorescent duty cycle (absorption
 61 followed by a spontaneous emission process) of
 62 $\Gamma = (Ns)/(\tau_f(1+s)) \simeq 2 \times 10^{13} \text{s}^{-1}$ with a saturation of
 63 the dye of $s = 2$ estimated from the experimental laser
 64 intensity.

65 The transmitted rays with angle of incidence smaller
 66 than i_c , form an Arago spot in the lower index medium.
 67 However, it is not so easy to find the trap location exper-
 68 imentally. To determine the position of the totally reflected
 69 Arago spot on the glass-liquid interface, we first image the
 70 spot using a 2 mW laser beam at several distances below
 71 the interface ($500 \mu\text{m}$ to $100 \mu\text{m}$, see Fig.1b), where the
 72 spot size is in the tens micrometer range. Then, by extrap-
 73 olation, we define a $10 \mu\text{m}$ -diameter area on the interface
 74 where we expect the total reflection of the Arago spot to
 75 occur. We concentrate the investigation of particles in this
 76 area only.

77 The rays diffracted by the disk impinge on the glass-
 78 liquid interface under different conditions. Close to the
 79 Arago spot, we have identified three types of rays: i) those
 80 impinging with an angle of incidence i higher than (but

81 very close to) the critical angle i_c (Fig. 2a). They con-
 82 tribute mostly to the trapping mechanism. ii) Those with
 83 $i > i_c$ (Fig. 2b) which also participate in the trapping but
 84 with a lesser extent. iii) Those with $i < i_c$ which do not
 85 participate in the trapping (Fig. 2c).

Trapping mechanism. – Let us have a closer look
 86 at the reflection of these rays and at the electromagnetic
 87 field close to the Arago spot. In Fig. 2a, the light rays
 88 lead to an Arago spot on the glass-liquid interface. These
 89 rays are totally reflected on the interface. They gener-
 90 ate an evanescent wave running away from the spot. The
 91 evanescent wave exists on a distance corresponding to the
 92 so-called Goos-Hänchen shift δ_{GH} [32]. In Fig. 2b, the
 93 Arago spot is above the glass-liquid interface. The asso-
 94 ciated rays are also under total reflection condition. The
 95 evanescent wave lasts on a smaller distance since δ_{GH} is
 96 smaller (the angle of incidence is higher). It forms a kind
 97 of donut centered on the Arago spot. In Fig. 2c, the rays
 98 are not totally reflected. However, because of the laws
 99 of refraction close to the critical angle, the transmission
 100 coefficient is very low and only a very little part of the
 101 light is transmitted [28]. Most of the rays are reflected
 102 with no evanescence. Those rays hardly contribute to the
 103 electromagnetic field in the liquid medium, close to the
 104 interface.
 105

106 Consequently, on the glass-liquid interface, in the liquid
 107 medium, the electric field is composed of outgoing evanes-
 108 cent waves centered on the Arago spot. Similar donut

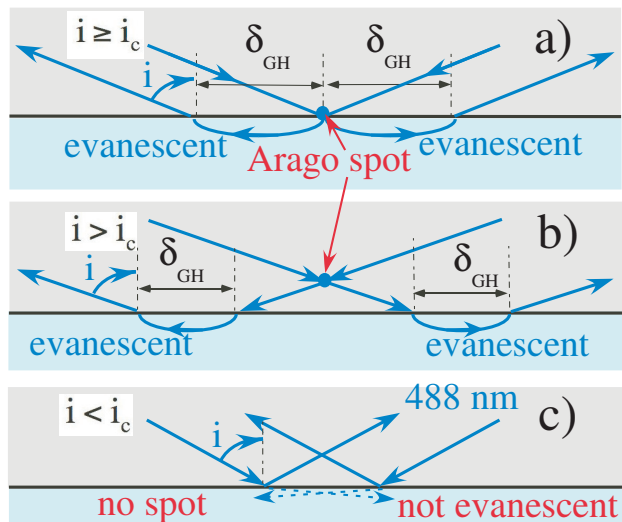


Fig. 2: Electromagnetic field at the glass-liquid interface near the Arago spot. Rays diffracted from the disk: a) that form a spot at the interface (angle of incidence i close to i_c , δ_{GH} : Goos-Hänchen shift); b) that form a spot above the interface (i higher than i_c), in a) and b), rays are totally reflected and generate outgoing evanescent waves; c) impinging on the interface with an angle smaller than i_c (they are partially reflected, with no evanescent wave). The dotted arrows correspond to the transmitted beam.

shape evanescent waves can be obtained using an occulted beam focused by a high numerical objective [15]. However, in that experiment, the optical beam results from a focusing and its size is thus limited by diffraction. It corresponds to a size of the order of a wavelength, whereas in our experiment, the beam size is smaller.

Nevertheless, the 470-nm light also plays a role. It is responsible for the trapping in the vertical direction. Each fluorescent particle within the flow interacts with this field. In a fluorescent cycle, the particle absorbs and gets excited. Since light carries linear momentum, due to momentum conservation, the particle recoils towards the glass-liquid interface. The radiation pressure force is estimated to $F_R = n_w \hbar k \Gamma = 3.3 \times 10^{-14}$ N, where \hbar is the reduced Planck constant and k is the wavevector. It acts on all the particles all along the channel, which therefore flow just underneath the glass-liquid interface. The electrostatic repulsion prevents them to stick to the glass, and keeps them away at a fraction of hundreds of nanometer distance [33]. Thereafter, particles fluoresce and recoil in a random direction.

What is then the trapping mechanism in the horizontal plane? It couldn't be via gradient forces. Compared with the previous experiments that trap particles in 3D using evanescent waves [15–17], our particles are 10 times smaller and the light intensity of the Arago spot is 10^{-5} times smaller. Then, the gradient force falls below 10^{-21} N. Actually, when the particle is close to the Arago spot, the 470 nm-light still enlightens it. After excitation, it

can either fluoresce as described before, or emit a stimulated photon in the evanescent wave at 488 nm (Fig. 3). This photon has exactly the same characteristics as the photons in the evanescent wave. The photon momentum is thus always directed outward from the spot (Fig. 2a and 2b). Because of linear momentum conservation, the particle is pushed towards the spot (Fig. 3a and 3c). This leads to a trapping force in the horizontal plane, with a capture range of about $r_t = 125$ nm. At the Arago spot position, the force cancels (Fig. 3b).

Small particles have already been trapped using focused super-oscillating beams [34]. However, the trapping mechanism they described is based on the dipolar force that strongly decreases when decreasing the trapped particle size. Besides, in this super-oscillating beam, a side lobe emerges very close to the fundamental lobe. This side lobe is much more intense than the fundamental one. Then, for very small beams, particles may be trapped in the side lobe instead of the fundamental one. That may be detrimental to reach small trap sizes. Moreover, whereas their trapping mechanism is very efficient in 2D, it is less efficient in the direction of the focusing of the beam, with a trapping size in the micrometer range as for optical tweezers. This is not the case of our trap where the trapping volume is the same in the three dimensions.

Results. – An example of a single trapped particle is shown in Fig. 4 (Fig. 4e to 4i). We fit the fluorescent signal of the particle with a Gaussian distribution intensity, and we assimilate the centre of the Gaussian with the centre of the particle [35], with 15 nm precision. Such a trajectory appears in Fig. 4m and 4n. During the trapping, the particle exhibits a Brownian like motion inscribed within a circle corresponding to the size of the trap. The position of the particle within the trap doesn't reflect the trapping potential of the light that is supposed to be harmonic. We will focus on the motion of the particle in the trap below (see end of following section). The trapping volume thus consists of a-125-nm radius cylinder in the horizontal plane whose height is limited by the penetration depth of the evanescent wave, i.e. about 200 nm.

In order to check whether the particle could be trapped by the gradient force instead of the stimulated emission force, we have performed the following experiment. We have replaced the 488 nm laser by a 404 nm laser. The fluorescein molecules cannot emit a photon in a stimulated way at this wavelength. However, for the same laser power, the gradient force is unchanged. We haven't noticed any particle trapping. This reinforces the stimulated emission hypothesis.

Discussion. –

Magnitude of the force. Let us evaluate the magnitude of the trapping force. To this purpose, we have to estimate the number of stimulated photons involved in the experiment. This can be performed via evolution equations [36].

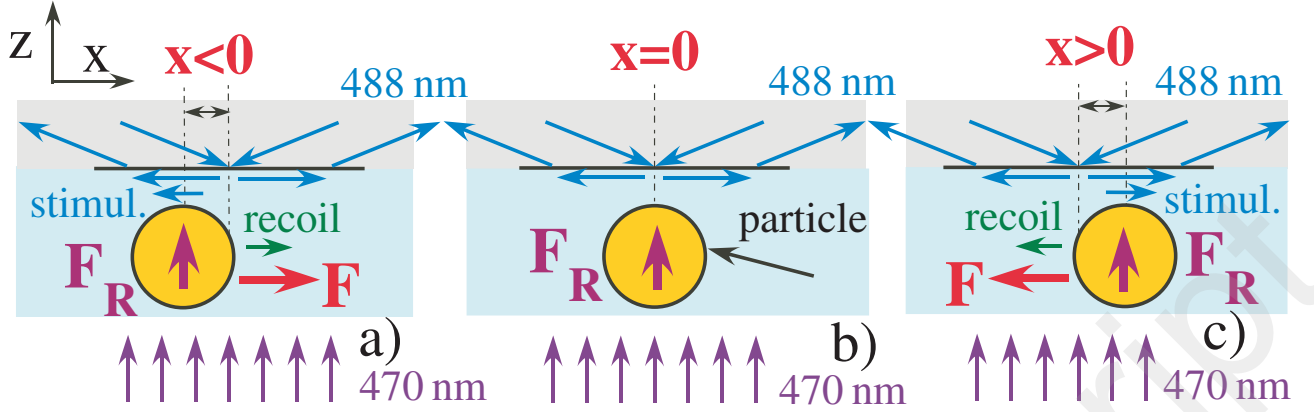


Fig. 3: Trapping mechanism. The radiation pressure force F_R from the 470 nm light (vertical arrows), pushes the particle in the upward direction, leading to a vertical trapping. In the horizontal plane, a) at a distance $x < 0$ from the spot, the excited particle, emits light in a stimulated way in the evanescent wave that goes out from the spot (horizontal arrows). Due to momentum conservation, the particle recoils towards the spot, leading to a spring force F . b) At the spot location $x = 0$, stimulated emission in both directions compensates. There is no resultant force. c) When $x > 0$, the effect is reversed compared to a). The particle is pushed towards $x = 0$.

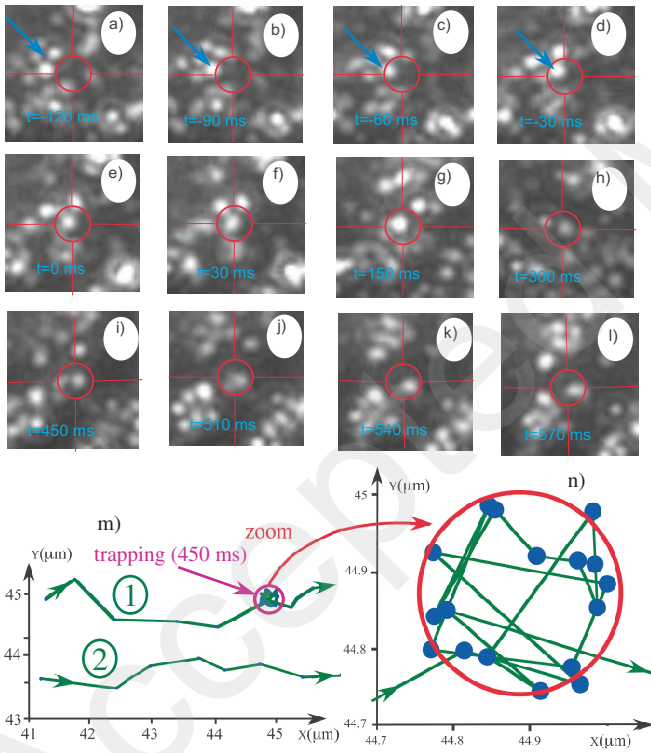


Fig. 4: Pictures of a trapped particle and particle trajectory. a) to d) Particle before trapping. The blue arrows point toward the particle. e) to i) Trapped particle (trapping period 450 ms). j) to l), particle escape. The red $3 \mu\text{m}$ -diameter circle highlights the trapping zone (much larger than the trap). m) Trajectory of a trapped particle before, during and after trapping (label 1). Trajectory of a non-trapped particle (label 2). n) Zoom of the particle trajectory during trapping. The diameter of the purple circle corresponds to the horizontal trap dimension.

Experimentally, we observe a decrease of the fluorescence of the trapped particle by about 2/3 compared with the non-trapping period. It then recovers its initial fluorescent rate when leaving the trap, in a way similar to the selective deactivation of fluorophores in STED microscopy [37]. In order to explain this decrease, let us write a simplified detailed balancing at thermal equilibrium of the absorption and emission process [38] in a cycle,

$$An_e + Bn_e\rho(\nu) - Bn_g\rho(\nu_0) + Cn_e = 0 \quad (2)$$

where A and B are the so-called Einstein coefficients, n_g and n_e are the populations of the ground and excited states of the particle ($n_g + n_e = 1$), respectively, and $\rho(\nu_0)$ and $\rho(\nu)$ are the spectral density energies of light at 470 nm and at 488 nm, respectively. Cn_e corresponds to non radiative decay from the excited state. The first term in Eq. 2 (An_e) accounts for the spontaneous emission, the second one ($Bn_e\rho(\nu)$) accounts for the stimulated emission at 488 nm, and the third term ($Bn_g\rho(\nu_0)$) accounts for the absorption of light at 470 nm. In the absence of the Arago spot, Eq. 2 leads to $An_e^0 - Bn_g^0\rho(\nu_0) + Cn_e^0$. The superscript accounts for the populations without the Arago spot.

Let us call δ the ratio between the spectral energy densities at 488 nm and at 470 nm ($\delta = \rho(\nu)/\rho(\nu_0)$), and α the decrease of the fluorescence due to the spot $\alpha = n_e/n_e^0$. Straightforward calculations lead to $n_e^0 = (1 - \alpha)/(\alpha\delta)$. In our experiment, $s = 2$, $n_e^0 = 2/3$. The light intensity at 470 nm and at 488 nm are nearly the same ($\delta = 1$), leading to $\alpha = 3/5$. This value of α is about the value we found experimentally. Using this value of α , we can estimate the force due to stimulated emission. Indeed, pushing forwards the calculations, we find $Bn_e\rho(\nu) = 6/5Bn_e^0\rho(\nu_0)$, leading to $F = 6/5F_R = 4 \times 10^{-14}$ N.

This value of the force can be checked experimentally.

The mean value of the square of the position of a trapped particle evaluated from Fig. 4n is $\sqrt{\langle x^2 \rangle} \sim 10^{-7}$ m, assuming an harmonic potential. We estimate the temperature of the particle to be around $T = 323$ K due to heating, leading to a thermal agitation $k_B T = 4.5 \times 10^{-21}$ J, k_B being the Boltzmann constant. The equipartition theorem leads to a trap stiffness $\kappa = k_B T / \langle x^2 \rangle \sim 4 \times 10^{-7}$ N.m $^{-1}$ and a force $F \sim \kappa \sqrt{\langle x^2 \rangle} \sim 4 \times 10^{-14}$ N. This experimentally deduced value of the force thus validates the calculation of the trapping force using Eq. 2.

Trap lifetime. We have followed the trapping of 160 particles (Fig. 5). The trapping time depends on the flow velocity: the slower the flow velocity, the longer the trap lasts. To estimate the trap lifetime τ , several quantities have to be considered. The first one is the momentum diffusion [39], due to the random recoil following an absorption-spontaneous emission cycle. The momentum diffusion coefficient equals to $D = \hbar^2 k^2 \Gamma = 5 \times 10^{-41}$ J.kg.s $^{-1}$. Note that this momentum diffusion coefficient is different from the usual position diffusion coefficient defined by Einstein $D_e = k_B T / \gamma$, $\gamma = 6\pi a \mu$ being the friction coefficient and μ the dynamical viscosity. Indeed, the Einstein coefficient is relevant for a diffusion process in position, whereas, in our case, in order to estimate the trapping time, we have to consider the diffusion in the momentum space.

The second relevant quantity for the trap lifetime is the depth of the trapping potential U_0 . It equals the force F times the capture range ($r_t = 125$ nm), leading to $U_0 = 5 \times 10^{-21}$ J. The third term is the thermal agitation ($k_B T = 4.5 \times 10^{-21}$ J). Note that we consider the trapping in the horizontal plane only, the vertical trapping is due to the radiation pressure as already explained. The last term accounts for the friction with the flow (v being the flow velocity). The following equation then sets

$$\frac{1}{m} D \tau = U_0 - k_B T - \gamma v r_t, \quad (3)$$

At 323 K, $\mu = 0.53 \times 10^{-3}$ Pa.s. One finds $\gamma r_t = 1.2 \times 10^{-16}$ N.s. The damping ratio is $\gamma / (2\sqrt{m\kappa}) = 400$. One expects a linear variation of τ versus the flow velocity, which is indeed experimentally observed (Fig. 5b).

From this figure, the maximum trapping time is $\tau = 0.8$ s leading to a diffusion term $D\tau/m = 10^{-23}$ J, whereas $U_0 - k_B T = 5 \times 10^{-22}$ J. This more than one order of magnitude discrepancy could be explained by the following arguments: i) the potential U_0 and the thermal agitation are of the same order of magnitude. A variation of 8% of the trapping force F would lead to a decrease of $U_0 - k_B T$ by a factor of 5. ii) The spontaneous photon may undergo amplified spontaneous emission [40]. Then the step of the random walk in momentum space is multiplied by a number corresponding to the number of stimulated photons, leading to a dramatic increase of D . For example, 3 amplified spontaneous photons would lead to an increase of $(3 + 1)^2 = 16$ in the diffusion coefficient.

From Fig. 5, $v = 45 \mu\text{m.s}^{-1}$ corresponds to $\tau = 0$. The friction term then equals $\gamma v r_t = 5 \times 10^{-21}$ J. This is one order of magnitude higher than the other terms in Eq. 3. It has to be noted that this friction term is relative to the flow around the particle (v is the flow velocity). However, this flow velocity v is estimated from the fluorescent particles around the trapped particle. The trapped particle is close to the interface, at an estimated distance of 100 nm, whereas the non-trapped particles are at much higher distances. For example, in a Poiseuille flow of radius 15 μm , the velocity from 1.5 μm to 100 nm decreases by a factor of 10. The flow velocity in Fig. 5 is thus overestimated. Then, the experimental results agree with the model described by Eq. 3.

In order for the trapping to be efficient, the trapping potential should be around 10 times the thermal agitation [41]. In our experiment, the trapping potential is of the order of the thermal agitation, limiting the trap lifetime to 0.8 s at most (Fig. 5b). During this time, a laser pulse could be sent also via the optical fiber in order to induce a chemical reaction for the trapped particle. The particle would be glued to the substrate. Then, thanks to the microstage, the spot could be moved, another particle could be trapped. One can thus print a regular pattern of glued particles on the substrate.

Nevertheless, this trapping time is too low for the usual applications of optical traps. However, an increase of the 488 nm laser power by a factor of 10 would increase the intensity of the evanescent wave by a factor of 10 without reaching the damage threshold of the particles. The stimulated emission and thus the trapping force in the horizontal direction would increase accordingly. Besides, a greater 488 nm laser power will increase the stimulation emission process and thus reduces the population of the excited state of the fluorescent particles. It will thereby increase the radiation pressure force and the trapping in the vertical direction, and will lower the momentum diffusion. This would boost the trapping time to the hundreds of seconds range.

The motion of the particle inside the trap still needs to be addressed (see Fig. 4n). This motion may be due to temperature gradients [42] and self thermophoresis. Actually, For a trapped particle, in an absorption (mean wavelength $\lambda_1 = 470$ nm) spontaneous emission (mean wavelength $\lambda_2 = 550$ nm) cycle, the energy difference between the two wavelengths is $\Delta E = hc(1/\lambda_1 - 1/\lambda_2) = 6.1 \times 10^{-20}$ J, c being the light velocity. The number of cycles for trapped particles equals $\Gamma/3$ (see the paragraph about the discussion of the force). The power to be evacuated is of the order of $P = \Delta E \times \Gamma/3 \simeq 4 \times 10^{-7}$ W. The trapping region radius is $r_t = 125$ nm. The heat flux equation [43] across the surface limiting the trapping volume ($S = 4\pi r_t^2$, spherical symmetry), assuming a steady state flux for a mean particle position at the center of the trap, leads to a temperature gradient $\frac{\partial T}{\partial r} = \frac{P}{Sk} \simeq 3 \times 10^6$ K.m $^{-1}$, $k = 0.6$ W.m $^{-1}$.K $^{-1}$ being the thermal conductivity of water and r the radial distance. The drift velocity [44] is then

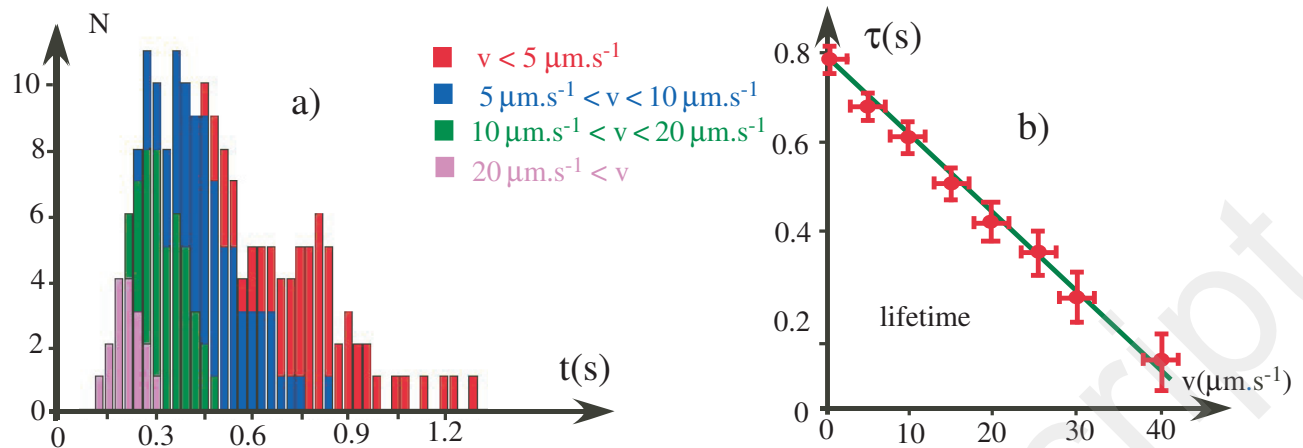


Fig. 5: Trap lifetime. a) Histogram of the trapping period for different flow velocities. N : number of particles that have been trapped. b) Variation of the mean trapping lifetime versus flow velocities. Red crosses: experimental data (the size of the cross represents the measurement uncertainty), green line: linear adjustment.

336 $u = D_T \frac{\partial T}{\partial r} \simeq 3 \mu\text{m.s}^{-1}$, $D_T = 10^{-8} \text{ cm}^2.\text{s}^{-1}.\text{K}^{-1}$ being
 337 the thermophoretic mobility. This drift velocity decreases
 338 as the particle reaches the edges of the trap.

339 The order of the magnitude of the velocity drift in the
 340 vicinity of the center of the trap is in the $\mu\text{m.s}^{-1}$ range,
 341 i.e., of the same magnitude as the flow velocity. This may
 342 prevent the particle to stay in the trap center. The particle
 343 seems to be located at the edges of the trap (see Fig. 4n).
 344 Although the radius of the trap is very small, this drift
 345 is one drawback of using fluorescent particles. This may
 346 also be a limiting factor of the measured lifetime. It is
 347 worth noting that similar position distributions have been
 348 encountered in the trapping of fluorescent particles, out of
 349 equilibrium [45, 46]. However these particles were Janus
 350 particles and the direction of the thermophoretic force is
 351 associated with their dissymmetry. The explanation in
 352 our case is different since we deal with spherical particles.

353 The trapped particles are 100 nm radius fluorescent particles.
 354 Since the trapping mechanism relies on stimulated
 355 emission, the magnitude of the force only depends on the
 356 fluorescent duty cycle Γ . This mechanism can be trans-
 357 posed to smaller particles (in the 10 of nanometer range or
 358 below). The number of fluorescent cycles would of course
 359 diminished, but the mass of the particle would also dimin-
 360 ish accordingly. The trapping efficiency would remain the
 361 same, whatever the size or the particle material. The only
 362 constraint is that the particles must absorb and reemit
 363 light.

364 **Conclusion.** – To conclude, we have described a new
 365 way to capture and trap fluorescent nanoparticles flow-
 366 ing inside a liquid. Compared with other techniques us-
 367 ing gradient forces, the laser intensity is rather low (in
 368 the W.cm^{-2} range). This enables the manipulation of
 369 nano-objects inside living organisms below photodamage.
 370 Besides, the trap position can be moved by sliding the
 371 occulting disk on the channel, in a way analogous to the

372 move of an immersion objective in a microscope. Although
 373 the experiment has been performed with blue lasers, it
 374 could be easily transposed to any wavelength, including
 375 infrared, depending on the transparency window of the ex-
 376 periment, just by changing the fluorescent particles. For
 377 example, such trapping system in the surface-plane could
 378 be used to trap fluorophores attached to organelles, viruses
 379 or even proteins in a lab on-a-chip integration. The size
 380 of conventional optical tweezers is too big to trap them
 381 efficiently. Such nanometer scale traps could then serve in
 382 transfection and single-and sub-cellular surgery [47] or for
 383 single-cell biopsies [48].

384 Conversely, looking at even smaller scales, the trap-
 385 ping mechanism evoked here, which is borrowed from laser
 386 trapping techniques [49], could trap several atoms or even
 387 molecules in a very small volume. In this later case, the
 388 experiment would hold in vacuum and the optical transi-
 389 tions of the atoms or molecules would replace the transi-
 390 tion of the dye molecules in the particle. It could thus
 391 be an alternative route towards Bose-Einstein condensa-
 392 tion [50] using a smaller number of atoms or molecules in
 393 a much smaller volume. Applications in the transport of
 394 cold atoms could also be considered [51]. Besides the tight
 395 confinement of the evanescent wave near the interface may
 396 open new opportunities in the study of non-linear optics
 397 in atomic media [52].

398 We acknowledge support from the Contrat Plan Etat
 399 Région CPER BUFFON. We would also like to thank
 400 an anonymous referee for its suggestions about the self-
 401 thermophoresis effect.

REFERENCES

- [1] GRIER D. G., *Nature*, **424** (2003) 810.

- 404 [2] KISHINO A. and YANAGIDA T., *Nature*, **334** (1998) 74. 466
- 405 [3] ETHER D. S. *et al*, *EPL*, **112** (2015) 44001. 467
- 406 [4] CAPITANIO M. and PAVONE S., *Biophys. J.*, **69** (2013) 468
- 407 1293. 469
- 408 [5] MARAGÒ O. M., JONES P. H., GUCCIARDI P. G., VOLPE 470
- 409 G. and FERRARI A. C., *Nat. Nanotechnol.*, **8** (2013) 807. 471
- 410 [6] WANG X., CHEN S., KONG M., WANG Z., COSTA K. D., 472
- 411 LI R. A. and SUN D., *Lab Chip*, **11** (2011) 3656. 473
- 412 [7] KIRKHAM G. R. *et al.*, *Sci. Rep.*, **5** (2015) 8577. 474
- 413 [8] CHOUDHARY D., MOSSA A., JADHAV M. and CECCONI 475
- 414 C., *Biomolecules*, **9** (2019) 23. 476
- 415 [9] DALY M., SERGIDES M. and CHORMAIC N. S., *Laser Pho-* 477
- 416 *ton. Rev.*, **9** (2015) 309. 478
- 417 [10] MAIA NETO P. A. and NUSSENZWEIG H. M., *Europhys.* 479
- 418 *Lett.*, **50** (2000) 702. 480
- 419 [11] SPESYVTSEVA S. E. S. and DHOLAKIA K., *ACS Photon-* 481
- 420 *ics*, **3** (2016) 719. 482
- 421 [12] MELZER J. E. and MCLEOD E., *ACS Nano*, **12** (2018) 483
- 422 12440. 484
- 423 [13] NEUMAN K. C. and BLOCK S. M., *Rev. Sci. Instrum.*, **75** 485
- 424 (2004) 2787. 486
- 425 [14] ALMAAS E. and BREVIK I., *J. Opt. Soc. Am. B*, **12** (1995) 487
- 426 2429. 488
- 427 [15] GU M., HAUMONTE J.-B., MICHEAU Y., CHON J. W. N. 489
- 428 and GAN X., *Appl. Phys. Lett.*, **84** (2004) 4236. 490
- 429 [16] GANIC D., GAN X. and GU M., *Opt. Express*, **12** (2004) 491
- 430 5533. 492
- 431 [17] YOON Y. Z. and CICUTA P., *Opt. Express*, **18** (2010) 493
- 432 7076. 494
- 433 [18] EMILE O., EMILE J. and TABUTEAU H., *EPL*, **116** (2017) 495
- 434 64003. 496
- 435 [19] NOVOTNY L., BIAN R. X. and XIE S., *Phys. Rev. Lett.*, 497
- 436 **79** (1997) 645. 498
- 437 [20] VOLPE G., QUIDANT R., BADENES G. and PETROV D., 499
- 438 *Phys. Rev. Lett.*, **96** (2006) 238101. 500
- 439 [21] JUAN M. L., RIGHINI M. and QUIDANT R., *Nat. Photon-* 501
- 440 *ics*, **5** (2011) 349. 502
- 441 [22] CROZIER K. B., *Light Sci. Appl.*, **8** (2019) 35. 503
- 442 [23] KOTSIFAKI D. G. and CHORMAIC S. N., *Nanophot.*, **8** 504
- 443 (2019) 1227. 505
- 444 [24] KLAR T., PERNER M., GROSSE S., VON PLESSSEN G., 506
- 445 SPIRKL W. and FELDMANN J., *Phys. Rev. Lett.*, **80** (1998) 507
- 446 4229. 508
- 447 [25] TANG X., ZHANG Y., SU W., ZHANG Y., LIU Z., YANG 509
- 448 X., ZHANG J., YANG Y. and YUAN Y., *Opt. Lett.*, **44** 510
- 449 (2019) 5165. 511
- 450 [26] GRIGORENKO A. N., ROBERTS N. W., DICKINSON M. R. 512
- 451 and ZHANG Y., *Nat. Photonics*, **2** (2008) 365. 513
- 452 [27] GALLOWAY C. M., KREUZER M. P., AÇIMOVIĆ S. S., 514
- 453 VOLPE G., CORREIA M., PETERSEN S. B., NEVES- 515
- 454 PETERSEN M. T. and QUIDANT R., *Nano Lett.*, **13** (2013) 516
- 455 4299. 517
- 456 [28] HECHT E., *Optics* (Addison-Wesley, San Fransisco) 2001. 518
- 457 [29] EMILE O. and EMILE J., *Appl. Opt.*, **59** (2020) 1678. 519
- 458 [30] SQUIRES T. M. and QUAKE R. S., *Rev. Mod. Phys.*, **77** 520
- 459 (2005) 977. 521
- 460 [31] SCHNEIDER C. A., RASBAND W. S. and ELICEIRI K. W., 522
- 461 *Nat. Methods*, **9** (2012) 671. 523
- 462 [32] LE FLOCH A., EMILE O., ROPARS G. and AGRAWAL G., 524
- 463 *Sci. Rep.*, **7** (2017) 9083. 525
- 464 [33] ILER, *The Chemistry of Silica* (Wiley, New York) 1979. 526
- 465 [34] SINGH B. K., NAGAR H., ROICHMAN Y. and ARIE A., 527
- Light Sci. Appl.*, **6** (2017) e17050. 528
- [35] YILDIZ A., FORKEY J. N., MCKINNEY S. A., HA T., 529
- GOLDMAN Y. E. and SELVIN P. R., *Science*, **300** (2003) 530
2061. 531
- [36] VERDEYEN J. T., *Laser electronics, 3rd Ed.* (Prentice 532
- Hall, New York) 2001. 533
- [37] HELL S. W. and WICHMANN J., *Opt. Lett.*, **19** (1994) 534
780. 535
- [38] EINSTEIN A., *Verh. Deutsch. Phys Gesell.*, **18** (1916) 318. 536
- [39] COHEN-TANNOUJJI C., DUPONT-ROC J. and GRYNBERG 537
- G., *Atom-Photon Interactions, Basic Processes and Ap-* 538
- plications* (Wiley-VCH) 1998. 539
- [40] DEMCHENKO A. P., *Introduction to fluorescence sensing* 540
- (Springer Science + Business Media BV) 2008. 541
- [41] ASHKIN A., DZIEDZIC J. M., BJORKHOLM J. E. and CHU 542
- S., *Opt. Lett.*, **11** (1986) 288. 543
- [42] BRAUN D. and LIBCHABER A., *Phys. Rev. Lett.*, **89** (2002) 544
188103. 545
- [43] SEARS F. W., YOUNG H. D. and ZEMANSKY M.W., *Uni-* 546
- versity Physics 7th Ed.* (Reading M. A., Addison-Wesley) 547
1987. 548
- [44] BRAIBANTI M., VIGOLO D. and PIAZZA R., *Phys. Rev.* 549
- Lett.*, **100** (2008) 108303. 550
- [45] MOYSES H., PALACCI J., SACANNA S. and GRIER D.G., 551
- Soft Matter*, **12** (2016) 6357. 552
- [46] SHEN C. and OU-YANG H. D., *Proc. SPIE, Optical Trap-* 553
- ping and Optical Micromanipulation XVI*, **11083** (2019) 554
- . 555
- [47] VILLANGCA M., CASEY D. and GLÜCKSTAD J., *Biophys.* 556
- Rev.*, **7** (2015) 379. 557
- [48] NADAPPURAM B. P., *et al.*, *Nat. Nanotechnol.*, **14** (2019) 558
80. 559
- [49] PHILLIPS W. D., *Rev. Mod. Phys.*, **70** (1998) 721. 560
- [50] BURT E. A., GHRIST R. W., MYATT C. J., HOLLAND 561
- M. J., CORNELL E. A. and WIEMAN C. E., *Phys. Rev.* 562
- Lett.*, **79** (1998) 337. 563
- [51] COUVERT A., KAVALEC T., REINAUDI G. and GUERY- 564
- ODELIN D., *EPL*, **83** (2015) 13001. 565
- [52] KUMAR R., GOKHROO V., DEASY K. and CHORMAIC S. 566
- N., *Phys Rev. A*, **91** (2015) 053842. 567